TIME REVERSAL IN ELASTODYNAMICS AND APPLICATIONS TO STRUCTURAL HEALTH MONITORING

Conference Paper · May 2015

CITATIONS
2

READS
166

3 authors:

Christos Panagiotopoulos
Foundation for Research and Technology - Hellas
42 PUBLICATIONS **482** CITATIONS
SEE PROFILE

Ioannis Petromichelakis
Columbia University
13 PUBLICATIONS **28** CITATIONS
SEE PROFILE

Chrysoula Tsogka
University of California, Merced
116 PUBLICATIONS **2,173** CITATIONS
SEE PROFILE

COMPDYN 2015
5th ECCOMAS Thematic Conference on
Computational Methods in Structural Dynamics and Earthquake Engineering
M. Papadrakakis, V. Papadopoulos, V. Plevris (eds.)
Crete Island, Greece, 25–27 May 2015

TIME REVERSAL IN ELASTODYNAMICS AND APPLICATIONS TO STRUCTURAL HEALTH MONITORING

Christos G. Panagiotopoulos [1], **Yiannis Petromichelakis**[1] **and Chrysoula Tsogka**[1,2]

[1]Institute of Applied & Computational Mathematics
Foundation for Research and Technology Hellas, Heraklion, Greece

[2] Department of Mathematics and Applied Mathematics
University of Crete, Heraklion, Greece
e-mail: tsogka@uoc.gr

Keywords: Elastic wave propagation, time reversal, source localization, damage detection, structural health monitoring, finite element method.

Abstract. *In structural health monitoring, detection of localized damage can be achieved by exploiting recorded signals at a limited number of sensors within the structure. Here we propose the localization of damage using an array of sensors as a computational time-reversal mirror (TRM). Time reversal (TR) is a physical process that exploits the time reversibility of wave equations and achieves re-focusing of the wave on the source of its origin by sending back, reversed in time, the signals recorded on an array of transducers. TR was originally introduced by Mathias Fink and his group and has several applications ranging from medical imaging to telecommunications [14].*

In the present work, we perform time reversal numerically in order to effectively detect and localize defects in a bounded two-dimensional elastic domain. This is a generalization of a respective time-reversal implementation in an acoustic medium [12]. The solid contains a number of N_r sensors which can act as sources as well. Our data is the response matrix of the scattered field, that is, the difference between the total field obtained in the damaged structure and the incident field corresponding to the response in the healthy structure.

Numerical solution of the wave propagation problem is performed using a mixed finite element formulation in terms of the velocity and stress fields [6]. In order to dissociate the response caused by N_d different defects, we apply the singular value decomposition (SVD) of the response matrix, while back-propagation of the projection of each singular vector corresponding to a non-zero singular value is performed in order to highlight each defect separately.

1 Introduction

An important component of several approaches in the design and construction of structural health monitoring systems are methods to efficiently identify and localize damage. Response recordings by sensors placed on a structure are often used to monitor the structure's integrity and to detect the appearance of damage [23]. Detection of damage can be done by comparing the response of the structure in its reference state with that recorded in the damaged state. Imaging of the damage, however, needs more sophisticated procedures. In this paper, we consider this query using time reversal imaging procedures of elastic waves propagating in bounded domains. Numerical back propagation of the recorded response will focus on defects' locations, since a defect behaves as a secondary source. The difficulty is that we do not know the time at which this secondary source will be activated. This time corresponds to the time that is needed for the incident wave to propagate from the source to the defect. An indication of the refocusing time can be obtained by the bounded variation norm of the TR field as in [12]. Here we propose to monitor the energy density function instead of the norm of the displacement, since it is a natural physical quantity and seems to give better numerical results.

Time reversal consists of two steps: a forward and a backward propagation one. In the forward propagation step, waves are emitted from some source and travel through the medium. During this step the wave-field is being recorded by one or more receivers. In the backward step, the previously recorded signals are reversed in time and they are rebroadcasted from their respective receiver positions. Wave paths that were traversed in the forward propagation step are now reproduced in the backward one [3]. Ideal conditions for the time reversal process would be those corresponding to the case where receivers fill the whole medium (or its entire boundary), recording the field and its derivatives [15], without any noise [16]. The time *reversibility* is based on the spatial *reciprocity* (symmetry in engineering) and the time reversal *invariance* (under the transformation $t \rightarrow -t$) of linear wave equations.

The time reversal technique has been recognized in recent years, because of its robustness and simplicity, as a quite appealing approach to resolve source localization problems. This branch of inverse problems finds numerous applications in several fields, e.g., medicine, telecommunications, underwater acoustics, seismology and engineering structures. Time reversal, with full or partial information, has been mathematically justified considering energy estimates for the wave equation [5], utilizing the Green's function properties [9] or modal analysis [17].

Numerical time reversal for elastic media has been considered in [11, 25] while experimental results are reported in[24, 21, 20]. The DORT (french acronym for decomposition of the time reversal operator) method applied to elastic wave scattering can be found in [4]. It has been shown that time reversal imaging can be also used in dissipative elastic media [2], which is important since any real structural system exhibits some damping.

In this paper we describe the numerical implementation of time reversal in elastic media and carry out simulations in order to assess the effectiveness of this process in damage identification problems. In general, we assume that response is recorded on N_r sensors, belonging in $\Omega_r \in \Omega$, while excitation is assumed to be produced by N_s source points forming $\Omega_s \in \Omega$. These two subspaces may be totally separated, coincide or just have an overlap. The described methodology can be applied to sensors that form an array, as well as to a distributed sensor configuration. For simplicity of presentation, we focus our attention on an array configuration where sources and receivers are collocated.

2 The time reversal process

Time reversal forward step In structural health monitoring (SHM) the forward step of TR corresponds to a physical process where the data response matrix is collected on a set of sensors located at $\boldsymbol{x}_r$, $r = 1, \ldots, N_r$. Each column of the response matrix corresponds to the response received at all sensors $\boldsymbol{x}_r$ and in all directions $i = x, y$ when a source point emits a pulse from the location $\boldsymbol{x}_s$ in a specific direction. In our case, the forward step is numerically simulated. A source located at $\boldsymbol{x}_s$ emits a pulse in the direction $\boldsymbol{e}_i$ and the response is recorded at the receiver locations $\boldsymbol{x}_r$. We consider a linear elastic material filling a bounded domain Ω with Dirichlet boundary conditions on its boundary $\partial\Omega$,

$$\begin{aligned}
&\rho\frac{\partial^2\boldsymbol{u}}{\partial t^2}(\boldsymbol{x},t) - \operatorname{div}\sigma\left(\boldsymbol{u}(\boldsymbol{x},t)\right) = \delta(\boldsymbol{x}-\boldsymbol{x}_s)\boldsymbol{e}_i f(t), (x,t)\in\Omega\times(0,T],\\
&\boldsymbol{u}(\boldsymbol{x},t) = 0, \qquad (\boldsymbol{x},t)\in\partial\Omega\times(0,T]\\
&\boldsymbol{u}(\boldsymbol{x},0) = 0, \qquad \boldsymbol{x}\in\Omega\\
&\frac{\partial\boldsymbol{u}}{\partial t}(\boldsymbol{x},0) = 0, \qquad \boldsymbol{x}\in\Omega
\end{aligned} \tag{1}$$

The displacement vector $\boldsymbol{u}$ is associated with the strain tensor by

$$\varepsilon_{ij}(\boldsymbol{u}) = \frac{1}{2}\left(\frac{\partial u_i}{\partial x_j} + \frac{\partial u_j}{\partial x_i}\right).$$

The stress tensor is given by Hooke's law

$$\sigma(\boldsymbol{u}) = C : \varepsilon(\boldsymbol{u}),$$

which connects stress to strains via the fourth order tensor of elastic moduli C (stiffness tensor). The inverse constitutive equation considering $A = C^{-1}$, the flexibility or compliance tensor, can be written as $\varepsilon = A\sigma$. Our numerical implementation is based on an equivalent formulation which consists in writing the elastodynamic problem as a first order hyperbolic system, the velocity-stress system,

$$\begin{aligned}
&\rho\frac{\partial\boldsymbol{v}}{\partial t} - \operatorname{div}\sigma = \delta(\boldsymbol{x}-\boldsymbol{x}_s)f(t)\boldsymbol{e}_i,\\
&A\frac{\partial\sigma}{\partial t} - \dot{\varepsilon} = 0,
\end{aligned} \tag{2}$$

for $(\boldsymbol{x},t)\in\partial\Omega\times(0,T]$ with $\dot{\varepsilon} = \frac{1}{2}\left(\frac{\partial v_i}{\partial x_j} + \frac{\partial v_j}{\partial x_i}\right)$. Here we omitted the dependence of the unknowns $\boldsymbol{v} = \partial\boldsymbol{u}/\partial t$ (the velocity vector) and the stress tensor σ on $(\boldsymbol{x},t)$. We should also add to our system, initial conditions $\boldsymbol{v}(t=0)=0$, $\sigma(t=0)=0$ and the boundary condition $\boldsymbol{v}=0$ on $\partial\Omega$. We solve the elastodynamic problem for all source locations $\boldsymbol{x}_s$, $s = 1, \ldots, N_s$ and the two directions $i = x, y$ and record the velocity $\boldsymbol{v}$ at all receiver locations $\boldsymbol{x}_r$, $r = 1, \ldots, N_r$. At the end of the forward step we have collected the response matrix $P(t)$ whose dimension at each time step is $2N_s \times 2N_r$.

Time reversal backward step The backward step of the time reversal process in the context of SHM applications is always performed numerically. However, it may be found in several alternative forms. For example, in [15] it is stated that one may force either just the field variable or the field variable and its first derivative recorded in the forward process. In the case of elastic wave propagation, a similar formulation is found in [25] where displacements' reversed time

history is imposed on points of sensors that record the response. Under this assumption the backward step would be given by the following initial-boundary value problem:

$$\begin{aligned}
&\rho\frac{\partial\tilde{\boldsymbol{v}}}{\partial t} - \operatorname{div}\tilde{\sigma} = 0, && (\boldsymbol{x},t)\in\partial\Omega\times(0,T],\\
&\tilde{\boldsymbol{v}}(\boldsymbol{x},t) = 0, && (\boldsymbol{x},t)\in\partial\Omega\times(0,T],\\
&\tilde{\boldsymbol{v}}(\boldsymbol{x},t) = \boldsymbol{v}(\boldsymbol{x},T-t), && (\boldsymbol{x},t)\in\Omega_r\times[0,T],\\
&\tilde{\boldsymbol{v}}(\boldsymbol{x},0) = 0, && \boldsymbol{x}\in\Omega,\\
&\sigma(\boldsymbol{x},0) = 0, && \boldsymbol{x}\in\Omega.
\end{aligned} \tag{3}$$

In [16], and some references therein, the wave is rebroadcasted through appropriate initial conditions. Alternatively, one can follow the approach used in [13] or [12] for acoustic waves, and adapt it to the case of linear elasticity that consists in solving the problem,

$$\begin{aligned}
&\rho\frac{\partial\tilde{\boldsymbol{v}}}{\partial t}(\boldsymbol{x},t) - \operatorname{div}\tilde{\sigma} = \sum_{q=1}^{N_r}\delta(\boldsymbol{x}-\boldsymbol{x}_q)\boldsymbol{v}(T-t), && (\boldsymbol{x},t)\in\Omega\times(0,T],\\
&A\frac{\partial\tilde{\sigma}}{\partial t} - \dot{\tilde{\varepsilon}} = 0, && (\boldsymbol{x},t)\in\Omega\times(0,T],\\
&\tilde{\boldsymbol{v}}(\boldsymbol{x},t) = 0, && (\boldsymbol{x},t)\in\partial\Omega\times(0,T],\\
&\tilde{\boldsymbol{v}}(\boldsymbol{x},0) = 0, && \boldsymbol{x}\in\Omega,\\
&\sigma(\boldsymbol{x},0) = 0, && \boldsymbol{x}\in\Omega.
\end{aligned} \tag{4}$$

In this case we set the reversed time recorded values of the field variable, as sources introducing right hand side loading terms on respective directions and spatial locations.

3 Damage identification

Several procedures for damage identification and localization, based on time reversal, have been proposed in the literature. In [1] an approach is considered for 2D scalar wave propagation problems, both forward and backward steps are assumed to take place in the cracked configuration of the medium. While for the forward step it is assumed that solution is obtained, or measured, for the correct cracked configuration, for the backward step a variety of cracked patterns is assumed, for each of them a wave propagation simulation is necessary, while the estimated cracked configuration is the one which gives the best refocusing on the source point. This procedure has been also extended to the case of elastic waves [18]. In [25] a technique similar with the methodology presented here has been proposed, however, in [25] there is no selectivity in the refocusing since the DORT method is not considered.

In our approach, we consider as data the impulse response matrix (IRM) of the scattered field, due to the damaged areas. This means that we assume that measurements of the response matrix in the healthy structure are available, and by subtracting them from the measured response in the damaged structure we obtain the scattered field.

3.1 Stopping criterion

During the backward step we expect the time reversed field to focus on the damaged area at some particular time, but this time is not known a priori. Based on the fact that we seek for a time at which the field is focused in space, stoping criteria based on the minimisation of appropriate norms of the field (e.g., Shannon entropy, bounded variation norm) have been proposed and successfully used in [12]. Another measure called “mathematical energy” has

been adopted in [18]. In the current work we choose to track the total energy defined by

$$\mathcal{E}(t) = \frac{1}{2}(A\sigma, \sigma) + \frac{1}{2}(\rho v, v), \tag{5}$$

or it's discrete analogue as presented in [7]. More precisely, we first define the discrete energy density and normalise it by its maximal value at each time step before computing its L^1 norm in space.

3.2 Multiple damaged areas

The DORT method [22] was developed as an imaging procedure capable to refocus selectively the field on different targets (defects). An extension of DORT for the detection of multiple linear and nonlinear scatterers has been presented recently in [4].

In this work, following the methodology developed in [8, 12], we propose to compute the singular value decomposition of the response matrix frequency by frequency, and then, by projecting the response matrix on the singular vectors that correspond to the largest singular values, we can selectively refocus the elastic field on different defects.

The IRM $P(t)$, is a $N_S \times N_R = (2N_s) \times (2N_r)$ matrix. In order to proceed, we first compute its Fourier transform and obtain $\widehat{P}(\omega)$. For each ω in the available bandwidth, we compute the singular value decomposition of $\widehat{P}(\omega)$ as,

$$\widehat{P}(\omega) = U(\omega)S(\omega)V^*(\omega) \tag{6}$$

where $U(\omega)$ is an $N_S \times N_S$ and $V(\omega)$ an $N_R \times N_R$ unitary matrix, while $V^*(\omega)$ is the conjugate transpose and $S(\omega)$ the $N_S \times N_R$ rectangular diagonal matrix with the non-negative real singular values on the diagonal. The N_S columns of $U(\omega)$ and the N_R columns of $V(\omega)$ are called the left and right singular vectors of $\tilde{P}(\omega)$ respectively. We can also write,

$$\widehat{P}(\omega) = \sum_{j=1}^{N_\sigma} \sigma_j(\omega) U_j(\omega) V^*(\omega), \tag{7}$$

where N_σ is the number of non-zero singular values. In the acoustic case and for small size scatterers there is an one-to-one correspondence between the scatterers and the significant singular values and vectors of the IRM. In the elastodynamic case, and even for small scatterers, each scatterer has two or more associated singular values (and vectors) [10]. For well separated defects, each singular value is associated with a specific damage, and the corresponding singular vector has the ability to re-focus the field on the specific defect allowing for distinguishing and illuminating even the weaker damaged areas.

To focus on different defects we compute the projection of each column $\widehat{P}^{(l)}$ of the response matrix on the k-th singular vector as

$$\widehat{P}_k^{(p)}(\omega) = \left(U_k^*(\omega)\widehat{P}^{(l)}(\omega)\right) V_k(\omega) \tag{8}$$

which is a column vector associated with the k-th singular value of the matrix . We may reconstruct by inverse Fourier transform the column vector $P_k^{(l)}(t)$, reverse it in time, and then send it back in the elastic medium. We expect this procedure to focus the energy of the elastic field on the defected areas of our domain.

4 NUMERICAL IMPLEMENTATION

The elastic wave propagation in two dimensions is solved with a mixed finite element formulation based on the discretization of the stress-velocity fields, expressed by the system of equations in eq.(2). Details of this mixed formulation may be found in [6]. The spatial discretization is compatible with mass-lumping, which leads to diagonal mass matrices, so that explicit time discretization schemes are obtained. For this specific formulation a rectangular spatial grid is necessary. Our methodology has been also implemented and tested using a finite element discretization of the displacement formulation [19], however, results are not presented here.

A specific distribution of sensors, spread over a line, that constitutes both sources and receivers is considered and called an array of sensors. The material of the rectangular domain is assumed to be that of steel with Lame's coefficients λ=$96.95GPa$ and μ=76.17GPa, while the mass density is ρ=7700kg/m^3. The pressure waves velocity is c_p=5689.9m/s and that of shear waves c_s=3145.2m/s. The size of the domain equals to L_x=62.747mm and L_y=69.037mm. The FEM mesh consists of 400×400 elements, while the array of the 21 equidistant sensors lies on a line of length 31.452mm, as shown in Figure 1. Damage is considered in the material as two distinct small areas of softer material given by a 10% degradation of both Lame's coefficients. The first of them is at location $(0.6L_x, 0.25L_y)$ and its area is equal to 0.1mm^2 while the latter one is located at $(0.6L_x, 0.75L_y)$ and its area is 0.4mm^2. In order to construct the response matrix for the scattered field, each dof, corresponding to a spatial location of a sensor and a specific direction x_1 or x_2, is excited, and response is computed and stored for all sensors and both directions. The function of excitation in time is that of a ricker-pulse with a central frequency of 1MHz. This corresponds to a wavelength for the shear waves of 3mm and a pressure wave wavelength of 5.7mm.

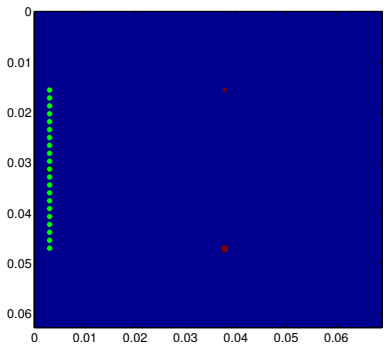

Figure 1: Geometry of elastic domain under consideration. Horizontal $y-$axis from left to right and vertical $x-$axis from top to bottom. Sensor array elements are shown with green dots and areas of damage are shown as red squares in the domain.

Plots in Figures 2 to 5, show results for the backpropagation steps using the field as recorded on the array, or after projecting it on the singular vectors corresponding to the first three singular values of the IRM. In all these figures we back propagate the column of the IRM that is obtained when the source is assumed to be on the central array element and exciting in the x-direction.

The left plot in each figure refers to the functional described by the integral,

$$\mathcal{I}(\mathbf{y}) = \int_0^T \mathcal{E}(\mathbf{y}, t)\, dt, \qquad \mathbf{y} \in \Omega, \tag{9}$$

where $\mathcal{E}(\mathbf{y}, t)$ is the energy density of the field on the spatial point $\mathbf{y}$ at time t, and T is the total duration time of the experiment. This functional is able to show the trajectories that the energy follows during the backward step of time reversal. As it can be seen these trajectories include the damaged areas. The plot in the middle is the time evolution of the energy criterion which may be used as an indicator for choosing the time instant at which the field focuses on the defects. The energy density of the time-reversed field at selected minima indicated by our criterion is shown on the right plot of each figure. We observe that by using the SVD we are able to detect and locate both damaged areas included in our domain.

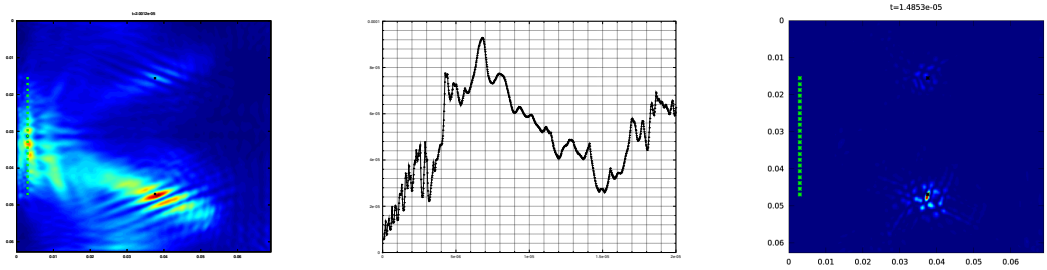

Figure 2: Backpropagation of the field recorded when the source is assumed to be on the central array element exciting in the x-direction.

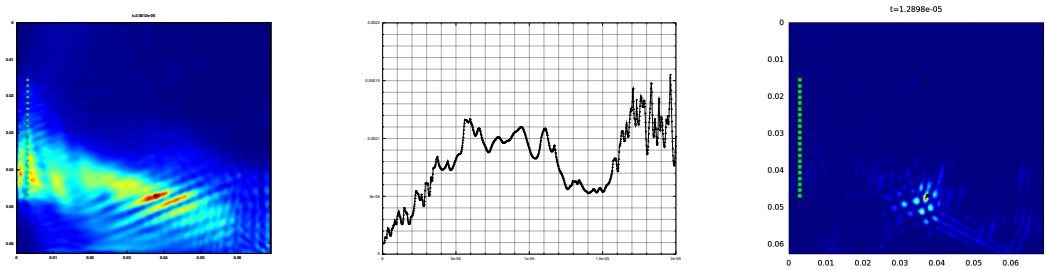

Figure 3: Backpropagating the same column of the response matrix as in Figure 2, but after projection on the singular vector corresponding to the first singular value.

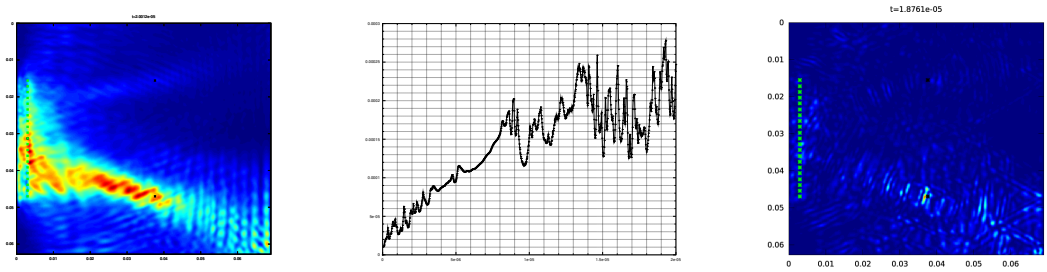

Figure 4: Backpropagating the same column of the response matrix as in Figure 2, but after projection on the singular vector corresponding to the second singular value.

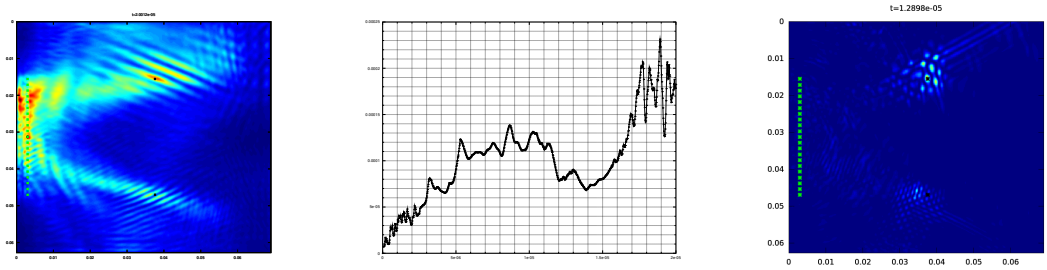

Figure 5: Backpropagating the same column of the response matrix as in Figure 2, but after projection on the singular vector corresponding to the third singular value.

5 CONCLUSIONS

We presented in this paper a computational methodology that uses the singular value decomposition of the array impulse response matrix in order to detect and localize defects in elastic materials. The energy density of the of the field seems a natural quantity to follow and a time-stopping criterion based on the L_1 norm of the normalized energy is proposed. The relevance of our methodology to SHM has been illustrated with numerical simulations.

REFERENCES

[1] Eyal Amitt, Dan Givoli, and Eli Turkel. Time reversal for crack identification. *Computational Mechanics*, 54(2):443–459, 2014.

[2] Habib Ammari, Elie Bretin, Josselin Garnier, and Abdul Wahab. Time-reversal algorithms in viscoelastic media. *European Journal of Applied Mathematics*, 24(04):565–600, 2013.

[3] Brian E Anderson, Michele Griffa, Carene Larmat, Timothy J Ulrich, and Paul A Johnson. Time reversal. *Acoustics Today*, 4(1):5–16, 2008.

[4] Ettore Barbieri and Michele Meo. Time reversal DORT method applied to nonlinear elastic wave scattering. *Wave Motion*, 47(7):452–467, 2010.

[5] Claude Bardos and Mathias Fink. Mathematical foundations of the time reversal mirror. *Asymptotic Analysis*, 29(2):157–182, 2002.

[6] E. Bécache, P. Joly, and C. Tsogka. A new family of mixed finite elements for the linear elastodynamic problem. *SIAM Journal of Numerical Analysis*, 39:2109–2132, 2002.

[7] Eliane Becache, Patrick Joly, and Chrysoula Tsogka. Fictitious domains, mixed finite elements and perfectly matched layers for 2-d elastic wave propagation. *Journal of Computational Acoustics*, 9(03):1175–1201, 2001.

[8] Liliana Borcea, George Papanicolaou, Chrysoula Tsogka, and James Berryman. Imaging and time reversal in random media. *Inverse Problems*, 18(5):1247, 2002.

[9] Hernán L Calvo, Rodolfo A Jalabert, and Horacio M Pastawski. Semiclassical theory of time-reversal focusing. *Physical review letters*, 101(24):240403, 2008.

[10] David H Chambers and James G Berryman. Time-reversal analysis for scatterer characterization. *Physical review letters*, 92(2):023902, 2004.

[11] Pier Paolo Delsanto, PA Johnson, Marco Scalerandi, and JA TenCate. Lisa simulations of time-reversed acoustic and elastic wave experiments. *Journal of Physics D: Applied Physics*, 35(23):3145, 2002.

[12] Gregoire Derveaux, George Papanicolaou, and Chrysoula Tsogka. Time reversal imaging for sensor networks with optimal compensation in time. *The Journal of the Acoustical Society of America*, 121(4):2071–2085, 2007.

[13] Oliver Dorn. Time-reversal and the adjoint method with an application in telecommunication. *arXiv preprint math/0412379*, 2004.

[14] Mathias Fink, Didier Cassereau, Arnaud Derode, Claire Prada, Philippe Roux, Mickael Tanter, Jean-Louis Thomas, and François Wu. Time-reversed acoustics. *Reports on progress in Physics*, 63(12):1933, 2000.

[15] Mathias Fink and Claire Prada. Acoustic time-reversal mirrors. *Inverse problems*, 17(1):R1, 2001.

[16] Dan Givoli. Time reversal as a computational tool in acoustics and elastodynamics. *Journal of Computational Acoustics*, 22(03), 2014.

[17] Dan Givoli and Eli Turkel. Time reversal with partial information for wave refocusing and scatterer identification. *Computer Methods in Applied Mechanics and Engineering*, 213:223–242, 2012.

[18] Izhak Levi, Eli Turkel, and Dan Givoli. Time reversal for elastic wave refocusing and scatterer location recovery. *Journal of Computational Acoustics*, 2014.

[19] Christos G Panagiotopoulos, Elias A Paraskevopoulos, and George D Manolis. Critical assessment of penalty-type methods for imposition of time-dependent boundary conditions in FEM formulations for elastodynamics. In *Computational Methods in Earthquake Engineering*, pages 357–375. Springer, 2011.

[20] Hyun Woo Park, Seung Bum Kim, and Hoon Sohn. Understanding a time reversal process in lamb wave propagation. *Wave Motion*, 46(7):451–467, 2009.

[21] Hyun Woo Park, Hoon Sohn, Kincho H Law, and Charles R Farrar. Time reversal active sensing for health monitoring of a composite plate. *Journal of Sound and Vibration*, 302(1):50–66, 2007.

[22] Claire Prada, Jean-Louis Thomas, and Mathias Fink. The iterative time reversal process: Analysis of the convergence. *The Journal of the Acoustical Society of America*, 97(1):62–71, 1995.

[23] Georgios E Stavroulakis. *Inverse and crack identification problems in engineering mechanics*, volume 46. Springer Science & Business Media, 2000.

[24] Chun H Wang, James T Rose, and Fu-Kuo Chang. A synthetic time-reversal imaging method for structural health monitoring. *Smart materials and structures*, 13(2):415, 2004.

[25] Xiao Dong Wang and GL Huang. Identification of embedded cracks using back-propagating elastic waves. *Inverse Problems*, 20(5):1393, 2004.